Int. J. Radiation Oncology Biol. Phys. Vol. 21, pp. 1063–1072
Printed in the U.S.A.

0360-3016/91 $3.00 + .00

● *Technical Innovations and Notes*

EVALUATION OF A TOTAL SCALP ELECTRON IRRADIATION TECHNIQUE

Charles M. ABLE, M.S.,* MICHAEL D. MILLS, PH.D.,* MARSHA D. MCNEESE, M.D.† AND KENNETH R. HOGSTROM, PH.D.*

The University of Texas, M. D. Anderson Cancer Center, Houston, TX 77030

A dosimetric evaluation of a total scalp electron-beam irradiation technique that uses six stationary fields was performed. The initial treatment plan specified a) that there be a 3-mm gap between abutted fields and b) that the field junctions be shifted 1 cm after 50% of the prescribed dose had been delivered. Dosimetric measurements were made at the scalp surface, scalp-skull interface, and the skull-brain interface in an anthropomorphic head phantom using both film and thermoluminescent dosimeters (TLD-100). The measurements showed that the initial technique yields areas of increased and decreased dose ranging from −50% to +70% in the region of the field junctions. To reduce regions of nonuniform dose, the treatment protocol was changed by eliminating the gap between the coronal borders of abutted fields and by increasing the field shift from 1 cm to 2 cm for all borders. Subsequent measurements showed that these changes in treatment protocol resulted in a significantly more uniform dose to the scalp and decreased variation of doses near field junctions (−10% to +50%).

Scalp irradiation, Electron beam, Dosimetry, Abutment dosimetry.

INTRODUCTION

Scalp lesions may occur consequent to such tumors as angiosarcoma, lymphoma, and melanoma (4, 9, 17, 20). Total scalp electron irradiation may be used to treat all these diseases, typically as an adjunct after surgical excision or chemotherapy, or alone as a definitive or palliative treatment (5). Radiotherapy is usually started within 6 weeks after surgery. Since the thickness of the scalp is only 4–6 mm (13), electrons are the modality of choice because of the high surface dose (when bolus is used) and finite range, which results in low dose (6) to the underlying brain tissues. Total scalp irradiation presents some difficult dosimetric problems because the scattering of electrons at oblique surfaces can create unusual dose distributions (8, 11, 14), and the effect of laterally scattered and backscattered electrons from the skull must be understood (19, 20). In addition, the use of secondary shielding results in a nonuniform dose distribution in regions where treatment fields must be abutted.

The total scalp electron-beam treatment at the M. D. Anderson Cancer Center consists of multiple stationary fields defined by customized secondary skin shielding in direct contact with the scalp. Standard treatment practice prescribes a total of 12 stationary fields. Initially, six fields are outlined on the patient's scalp using Castellani's paint with a cotton swab. Examples of such ports are seen on the human head phantom in Figure 1. There is a 3-mm gap between all adjacent fields; in clinical practice this is approximate because the secondary skin shielding was fabricated to exclude the field lines, which are approximately 3 mm. We used a standard electron applicator with customized inserts or blocking, which projected a field with at least a 2-cm margin beyond the field size as defined by the secondary skin shielding. The 2-cm criterion ensures that penumbra cast from the blocking within the standard applicator lies outside the treated area; this results in a sharp penumbra defined by secondary skin shielding and a uniform beam within its boundaries. A 6-mm thick slab of acrylic (polymethyl methacrylate) bolus is positioned approximately 5 mm above the surface on the central axis to increase the surface dose and to decrease the energy of the 7-MeV beam to approximately 5 MeV, thus reducing the depth of maximum dose (R_{100}), the therapeutic depth (R_{90}), and practical range (R_p). Theoretically, there will be an increased dose at depth in the field junction region caused by the overlapping of dose from the adjacent fields (12). The magnitude and distribution of dose in this region will be influenced by the angle of incidence of each beam at the field junction, as well as by sidescatter and backscatter

*Department of Radiation Physics.
†Department of Clinical Radiotherapy.
Reprint requests to: Kenneth R. Hogstrom, Ph.D., Department of Radiation Physics, Box 94, The University of Texas, M. D. Anderson Cancer Center, 1515 Holcombe Blvd., Houston, TX 77030.

Acknowledgement—This work was supported in part by National Cancer Institute grant CA-06294.
Accepted for publication 29 March 1991.

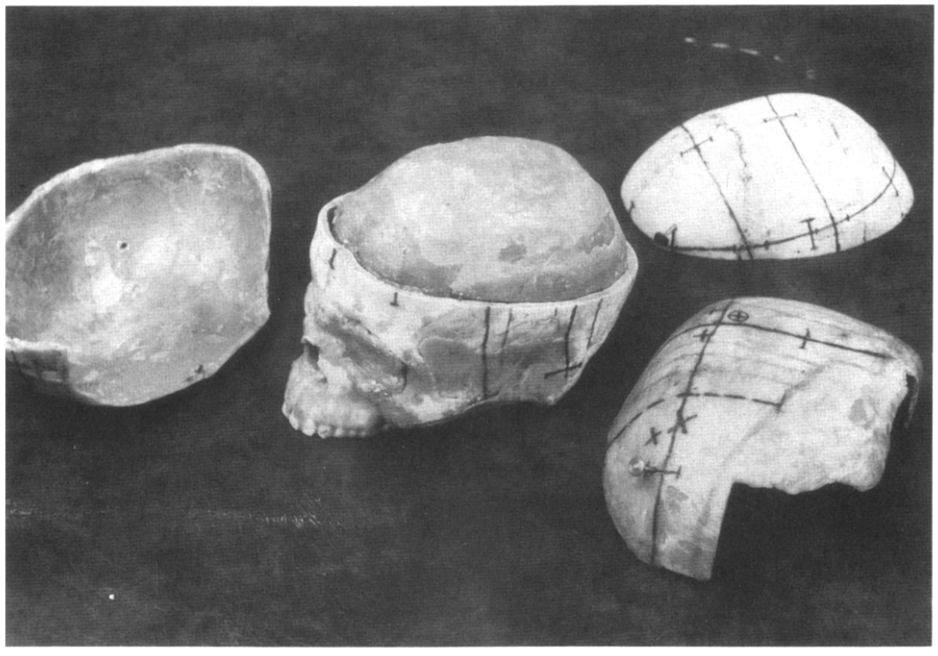

Fig. 1. Head phantom, constructed with a human skull and beeswax, with sections removed for display.

from bone (19). A 1-cm field shift was used to dilute the effect of dose heterogeneity in the field junction region. The field junctions were shifted 1 cm after 50% of the prescribed dose had been delivered. The total tumor dose ranges from 50 to 70 Gy (typically prescribed to the 95% depth dose) over 5.5 to 6.5 weeks (5). The dosimetric study of this technique resulted in a modified technique which greatly improved dose uniformity (2).

METHODS AND MATERIALS

Water phantom dosimetry

To achieve an acceptable entrance dose while maintaining the desired beam penetration, a 6-mm thick, acrylic slab bolus was placed perpendicular to a 7-MeV electron beam,* 5 mm above the surface. Measurements were performed in a water phantom to determine the central-axis characteristics of this specialized electron beam. A parallel plate chamber† was used to measure the central-axis depth-ionization curve. Depth-ionization data were converted to depth dose using Almond's equations (3), which corrected for the stopping power ratio at every depth. The beam's incident mean energy, $\overline{E}_o$, (1) was 4.8 MeV, with an R_p of 2.67 cm, a depth of maximum dose (R_{max}) of 0.9 cm, and R_{80} of 1.62 cm.

All experimental data were normalized such that 100% was the maximum dose on central axis in water (6-mm acrylic slab above water) for the 10 × 10-cm standard cone. A 0.6-cm^3 Farmer replacement cylindrical ion chamber,‡ operated at 300 V and fastened inside the electron collimator, served as an external monitor to correct for any fluctuations in machine output. This monitor chamber was present during all water and skull phantom measurements and was positioned so that the primary electron beam impinging on the phantom was not perturbed.

Head phantom setup technique

To evaluate the total scalp irradiation technique, an anthropomorphic head phantom was developed. This phantom was fabricated from a human skull and beeswax. The dehydrated skull was first submerged in agar to restore the bone to its proper physical density (7) of approximately 1.5 g cm^{-3} and then sealed with a thin wax coating. Beeswax was used to form the scalp and brain since its physical density (0.97 g cm^{-3}) and chemical composition (hydrocarbons) are close to those of human tissue (21). The wax was smoothed and shaped, forming a sturdy, removable wax scalp. The scalp thickness varied from 4–6 mm, simulating the human scalp (13). Figure 1 shows the resulting phantom with various sections removed. When delineating the treatment fields on the patient's scalp, a saggital line is drawn first. The saggital line should be drawn 1 cm to the left or right of the mid-saggital plane. Next, each hemisphere of the cranium is divided into three treatment fields (i.e., frontal, parietal-temporal, and parietal-occipital) by drawing two lines in the coronal plane. The coronal lines in the right hemisphere are shifted 1 cm from those of the left hemisphere so that no more than three portals will abut at any point along the saggital line

*Mevatron 77, Siemens Medical Laboratories, Concord, CA.
†PTW/Markus Chamber, Nuclear Associates, Carle Place, NY.
‡Model 2505/3B, Nuclear Enterprises, Fairfield, NJ.

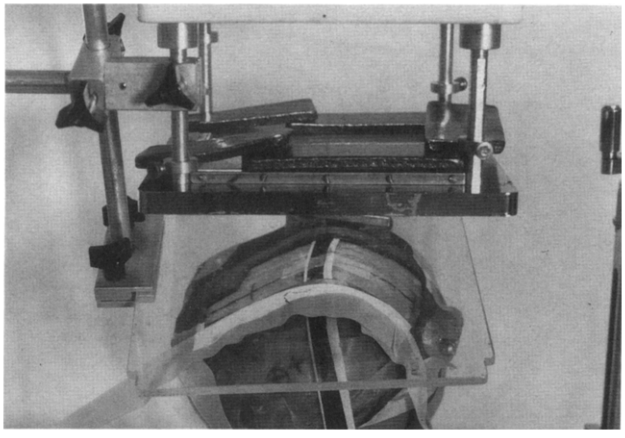

Fig. 2. View of irradiation geometry for left, central field. Note the custom collimation in the treatment applicator and the skin collimation. The acrylic bolus is supported by a holder and is perpendicular to central axis. The strip in the central portion of the field is a film on the scalp surface.

on a given treatment day. Halfway through treatment the coronal lines on the right and left hemispheres are switched.

Each of the six treatment fields was outlined on the phantom surface using a wax pencil. The head phantom was scanned by computed tomography (CT) in both the transverse and coronal planes, from which a transverse and two coronal planes were chosen for study. The planes were indicated on the surface of the phantom with a marking pen. A customized secondary skin shield was then fabricated from lead for each treatment field. The lead shields were 0.32-cm thick, corresponding to 3% transmission of 7-MeV electrons. Lead blocks were inserted in the standard electron applicator to produce an electron field which provided a 2-cm margin beyond the field size defined by the secondary skin shield.

Treatment setup is a two-step process. For each field the secondary skin shield must be accurately positioned on the head to define the treatment field. With the shield in place, the head must be positioned to reproduce the angulation or tilt of the head within the beam. The head was positioned so that the secondary shield was supported by the cranial anatomy and masking tape. Two bubble levels, mounted onto the skin shield and oriented perpendicular to one another during the initial setup, were used to facilitate subsequent reproducible setups of the head position in space. Gantry, table, and collimator rotation angles were chosen such that the beam entered perpendicular to a plane defined (approximately) by the edges of the field. If gantry rotation was too severe, masking tape was used to constrain the lead blocks in the applicator. By directing the beam perpendicular to the plane defined by the field edges, the air gap at the field edge was minimized and more uniform, thus introducing a more uniform dose distribution across the treatment field. A source-to-surface (SSD) point was chosen, usually at the geometric center of the field. The irradiation setup for the central, left lateral field is shown in Figure 2.

To achieve the therapeutic objective, we used a 6-mm acrylic slab bolus overlying the skin, increasing the surface dose from 72% to 90% or greater. Because the scalp is a sharply sloping surface, a flexible bolus lying on the surface is inadvisable. It would introduce dose irregularities, since bolus thickness increases by the secant of the angle. In addition, because of scatter, sloping surfaces introduce a self-bolusing effect resulting in a shortening of the R_{90} (8). Therefore, the slab acrylic bolus is used to maintain beam penetration throughout the field while delivering a high surface dose. The use of non-contact bolus requires skin collimation, and the rules regarding the use of skin collimation are: a) the projected light field defined by the 15 × 15-cm applicator (with blocks) should lie at least 1.5 cm (50%–90% penumbra width) outside the field defined by skin collimation, and b) the skin collimator should extend at least 3.0 cm outside the light field, resulting in electron scatter leakage being less than 2%. Details of this technique have been previously described (10).

In-phantom measurements were made along a curved path in both the transverse and coronal planes at the skin surface, scalp-skull interface, and skull-brain interface. The dose gradient across the scalp tissues was determined from the surface and scalp-skull measurements. The skull-brain measurements were made to verify that dose to the underlying brain tissues were not in the dose build-up region of the electron beam and to quantify the increased dose due to beam overlap.

Film dosimetry

The treatment technique was evaluated by film dosimetry. Film was used as the primary dosimeter because of its high spatial resolution and because it is relatively thin; its placement at the interface only minimally perturbs the setup. Special film packets used for this study had a total thickness of 1.2 mm, consisting of 1.5 × 30.5-cm strips of film,§ opaque paper, and black photographic tape. This film was chosen because of its linear dose (up to 25 cGy) (2, 3), verified by measurements at d_{max} in a polystyrene phantom. Film exposures were less than 25 cGy so that the net optical density was assumed directly proportional to dose (12). The dose to the film in the polystyrene phantom was the product of monitor units, dose per monitor unit in water, and the ratio of fluence in polystyrene to that in water (6, 16). The relative dose, measured by film in the head phantom, was determined from net optical density by:

$$D_{head}\ (\%) = \frac{(OD_{net}/mu)_{head}}{(OD_{net}/mu)_{water}} \times 100\ , \qquad (1)$$

§Kodak Industrex M2, Eastman Kodak Co., Rochester, NY.

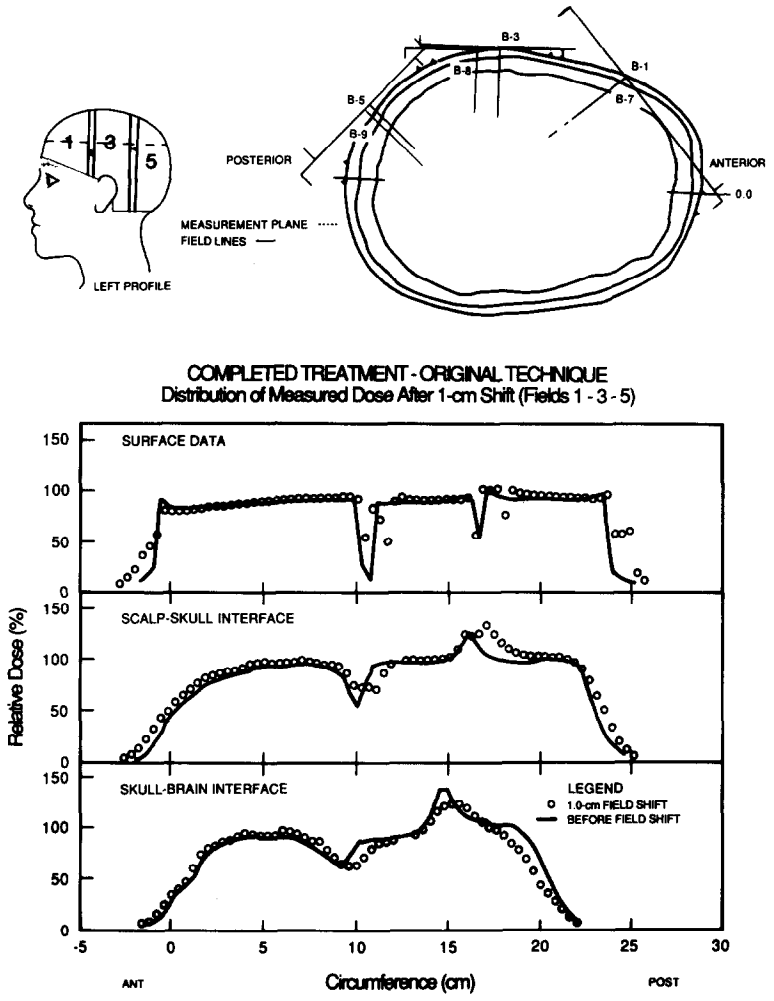

Fig. 3. Transverse plane dose distribution, fields No. 1, 3, and 5 were irradiated and then fields No. 7, 8, and 9 after 1.0-cm field junction shift. Film measurements made along the circumference at the surface, scalp-skull interface, and skull-brain interface. 7-MeV electrons; 6-mm acrylic at 98.9-cm source-to-acrylic distance; 100-cm SSD. Completed treatment — original technique. The solid line shows the distribution before the field shift with field lines not treated. The arrow indicates the field shift midway through the treatment.

where $(OD_{net}/mu)_{head}$ is the net optical density per monitor unit measured in the head phantom and $(OD_{net}/mu)_{water}$ is the net optical density per monitor unit (mu) at d_{max} in water. The latter is determined from the product of net optical density per monitor unit in the polystyrene phantom and the ratio of fluence in water to that in polystyrene (6). Note that this means that all dose measurements are relative to the maximum dose on central axis in a water phantom (given dose), as previously discussed.

Phantom measurements were made at the surface, the scalp-skull interface, and skull-brain interface in the measurement plane of interest. Each film was irradiated individually to obtain the profile across one, two, or three fields at the interface of interest. Figure 2 demonstrates the placement of the film on the surface defined by the intersection of the transverse plane with the left hemisphere of the head. All measurements were made in triplicate. Film exposed to a single field was irradiated to 15 monitor units to ensure that the optical density was within the linear portion of the dose-response curve. When the field junctions were moved, 1-cm or 2-cm shifts, each field was irradiated to 10 monitor units.

Thermoluminescent dosimetry

Point dose determination was accomplished with a thermoluminescent dosimeters (TLD-100) to verify our film dosimetry. Each TLD dosimeter consisted of approximately 27 mg of LiF TLD-100 powder enclosed in a sealed cellophane flat pack. The active volume of the dosimeter was approximately 3 × 3 × 1 mm thick. Each dosimeter was read approximately 24 hr after irradiation. Details of the dosimeter reading system have been described before (11). Multiple readings indicated a standard deviation of approximately ± 2%.

Accuracy and reproducibility of measurements

Three sets of film irradiated on the same day and developed simultaneously and one set of film irradiated on each

of three different days and developed separately were evaluated to determine the precision of the film data. The variation in relative dose in the central region of the field (where readings would not be affected by any alignment uncertainty) when films were processed simultaneously was less than ±2%. The variation in relative dose in the central region of the field when films were processed on separate days was less than ±4%. These results indicate that the precision of the film data over the course of this study was approximately ±4%.

The accuracy of the film measurements was evaluated by comparing film measurements with those of TLD-100 (flat pack) in the head phantom at the surface, scalp-skull interface, and skull-brain interface. The relative dose measured with film was accurate to within 3% of relative dose measured with TLD-100.

To evaluate the reproducibility of treatment setup, film strips were placed at the surface, scalp-skull interface, and skull-brain interface and irradiated simultaneously for a single field, resulting in data at all three levels for one treatment setup. The film strips were registered using small reference pins that penetrated the scalp, skull, and film. This measurement was repeated six times for each of the three different fields on the right side of the head phantom. The variation in the position of the edge of the field (approximately 50% of the central-axis dose) represented variation in the treatment setup. Changes in field positioning resulting from the misalignment of the secondary skin shielding were readily determined from the surface film measurements. Increasing misalignment at depth would indicate a problem in reproducibility of beam angulation. Any changes in field positioning resulting from the improper angulation of the head were recognized by the variation in the field edge at depth (skull-brain interface). The surface measurements indicated a total precision of approximately ±2 mm in field positioning. The skull-brain interface measurements indicated a total variation of approximately ±3 mm, which means that an additional variation of approximately ±1 mm was due to positioning of the angulation of the head phantom. These results indicate an overall uncertainty of ±3 mm in field positioning due to treatment setup.

RESULTS AND DISCUSSION

Results of original total scalp irradiation technique

Figure 3 shows the dose distribution in the transverse plane on the left side of the head, with a 1-cm junction shift midway through treatment. The straight ticmarks on the beam crossbar indicate the edges of the collimated beam; ticmarks above and below the bar correspond to the beams labeled above and below the bar. The triangular ticmarks on the surface of the phantom crossection indicate the position of the field lines defined by the skin collimation. The solid line in the graph illustrates the dose profiles resulting after the initial treatment (three fields), whereas the circles illustrate the dose profile resulting after the 1-cm field shift (six fields). Only the results for the total treatment will be reviewed. The surface dose ranged from approximately 87% to 93% of the given dose in the central region of each field. In the field junction regions, the dose decreased to as low as 50–74% of the given dose. These cold spots were due to the 3-mm gap (exclusion of the field demarcation lines) between abutting fields. At the scalp-skull interface the dose was approximately 95% of the given dose in the central region of each field. In the field junction region between fields 1 and 3, the geometric converging of the field edges does not produce sufficient dose overlap to compensate for the exclusion of these tissues from the treatment portals, resulting in a cold region of approximately 75%. In the field junction region between fields 3 and 5, the opposite is true; the dose overlap produces a hot region of approximately 125%. At the skull-brain interface, in the central region of each field, the dose varies from approximately 90% to 102%. The characteristics of the dose in the field junction regions are the same as measured at the scalp-skull interface. The minimum dose between fields 1 and 3 is 65%, and the maximum dose between fields 3 and 5 is 125%.

Figure 4 shows the dose distribution across fields 1 and 2 in the coronal plane, with a 1-cm junction shift midway through treatment (dashed line shown on the left profile). Again, the solid lines in the graph illustrate the dose profiles after the first half of the treatment, whereas the circles illustrate the dose profiles resulting after full treatment with the 1-cm field junction shift. Only the results for the total treatment will be reviewed. The surface dose measured across the central region of each field was approximately 100% of the given dose. Oblique beam incidence and the topology of the head in this region resulted in increased electron scatter under the edge of the secondary collimator, which increased the maximum surface dose in the field junction region to approximately 126%. The additional dose overlap at the scalp-skull interface produced a maximum dose of 170% in the field junction region. The dose in the central region of the fields at this interface was uniform at approximately 100%. A maximum dose of 140% in the field junction region was measured at the skull-brain interface. The dose overlap at this depth maintained a high dose in the field junction region, while beam penetration and increased electron fluence in the central region of the fields resulted in measured doses of 100% or less. It was not possible to measure the complete dose profile at the skull-brain interface in the coronal plane because of limitations imposed by the phantom design.

The magnitude of the dose in the field abutment volume indicated its being affected by the uncertainty in field positioning (±2–3 mm), as discussed previously. Another important point is that the dose on the surface and at depth in the field junction region (at field lines drawn in the sagittal plane, Fig. 4) was consistently high (≥ 100%). At field lines drawn in the coronal plane (solid lines shown on

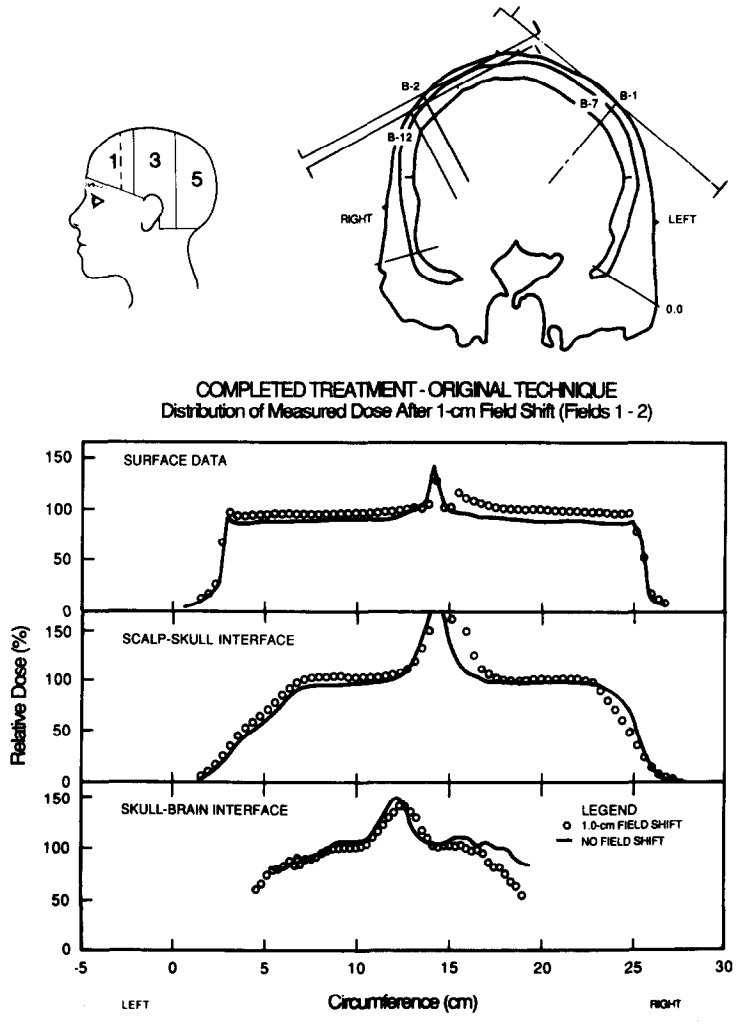

Fig. 4. Coronal plane dose distribution, fields No. 1 and 2 were irradiated, and, then fields No. 7 and 12 after 1.0-cm field junction shift. Film measurements made along the circumference at the surface, scalp-skull interface, and skull-brain interface. 7-MeV electrons; 6-mm acrylic at 98.9-cm source-to-acrylic distance; 100-cm SSD. Completed treatment — original technique. The solid line shows the distribution before the field shift with field lines not treated.

the left patient view, Fig. 3), the dose on the surface in the field junction regions was consistently low (≃ 50%). In addition, the dose overlap in the field junction region at depth did not compensate for the lack of direct irradiation of the field junction lines. These results illustrate the inadequacy of the 1-cm field junction shift. As a result of (a) the inconsistency, and therefore unpredictability, of dose in the field junction region, and (b) its deviation from the given dose, changes in treatment protocol were necessary.

Results of modified total scalp electron technique

The practice of excluding the field demarcation lines from the treatment field was reviewed first. The consistently high dose measured at the surface and scalp-skull interface along the field lines drawn in the sagittal plane indicated that the gap between abutted fields should not be reduced, since the dose is predictably high (Fig. 4). However, the dose was inconsistent for field lines drawn in the coronal plane. At the surface a cold spot was measured, whereas the dose at the scalp-skull and skull-brain interface varied (Fig. 3). To avoid a cold spot at the surface and scalp-skull interface, the field lines drawn in the coronal plane were included in the revised treatment field, that is, the approximately 3-mm gap was eliminated.

The practice of shifting the field junction lines 1 cm after 50% of the prescribed dose has been delivered was also reviewed. The objective of the field junction shift is to produce a more uniform dose distribution by overlapping a region of nonuniform dose (field junction) with a region of uniform dose (approximately 100%). Since the 1-cm shift did not accomplish this objective, a 2-cm shift was used.

Figure 5 shows the resulting dose distribution (circles) from the modified technique halfway through treatment (no gap, but junction not yet shifted) on the left side of the head in the transverse plane. For comparison, the solid lines in the graphs illustrate the dose distribution for the original technique with the 3-mm gap (lines were not treated, c.f. Fig. 1). The probability of cold spots on the

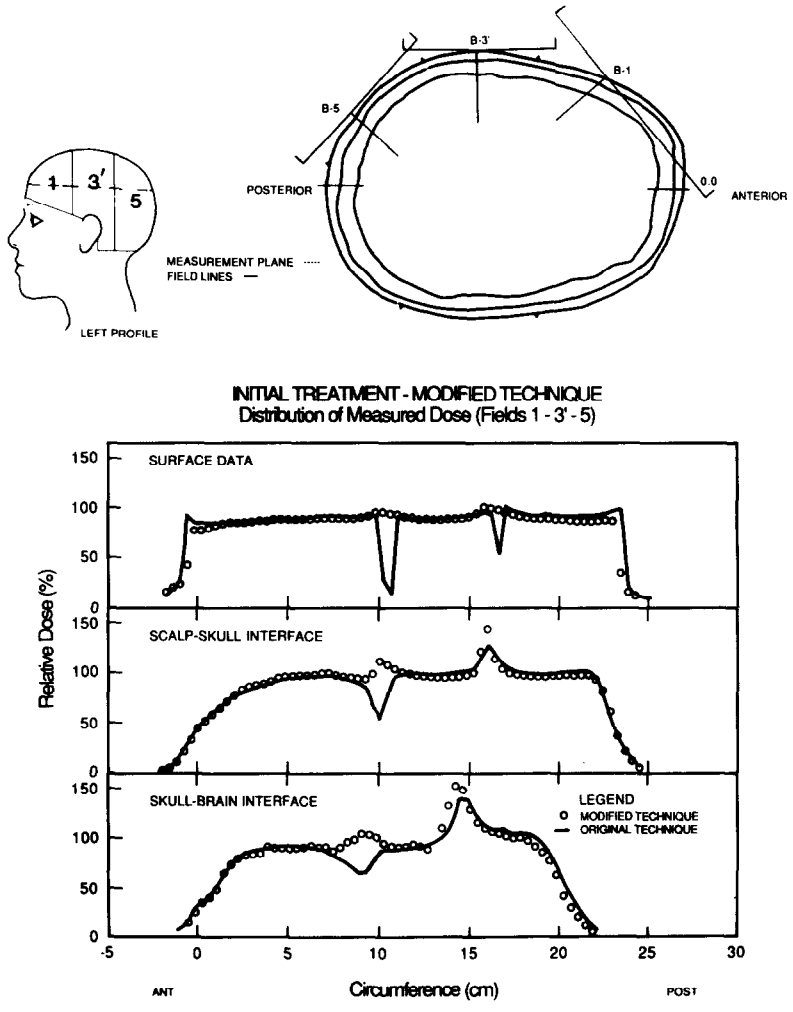

Fig. 5. Transverse plane dose distribution, fields No. 1, 3′, and 5. In field 3′ both field lines were treated. Film measurements made along the circumference at the surface, scalp-skull interface, and skull-brain interface. 7-MeV electrons; 6-mm acrylic at 98.9-cm source-to-acrylic distance; 100-cm SSD. Initial treatment — modified technique. The solid line shows the distribution from initial treatment using the original technique with field lines not treated (Figure 3).

surface is significantly reduced when the field lines are treated, although not completely eliminated since setup error still exists. The beam angles and electron scattering at depth ensure a dose of at least 100% at the scalp-skull interface by implementing this change in protocol. A hot spot dose of 150% is noted at the skull-brain interface. By inclusion of the lines, all cold spots are eliminated and the hot spots increased, now indicating a definite need for good edge feathering.

Results in the transverse plane of the complete treatment with the modified technique, now having a 2-cm field shift, are illustrated in Figure 6. For comparison, the solid lines in the graphs show the dose distribution resulting from our original technique, that is, having the 1-cm field shift with the 3-mm gap (field lines excluded from the treatment portals, c.f. Fig. 3). The 2-cm field shift data (circles) will be reviewed first and compared with data in previous figures. The surface dose is reasonably uniform, varying from 90% to 100%. The maximum dose at the scalp-skull interface after the 2-cm field shift (140%) was reduced only slightly from results without the field shift (Fig. 5) and is slightly greater than the maximum of the composite, original technique. The maximum dose at the skull-brain interface after the 2-cm field shift was reduced from 150% (Fig. 5) to 120%. When comparing the two distributions shown in Figure 6, one readily sees the somewhat higher and more uniform dose distribution across the scalp tissues produced by the modified technique.

Figure 7 illustrates the dose distribution measured in the coronal plane when using the modified and original techniques. The decrease in the magnitude of the maximum dose when using the modified technique is illustrated at the scalp-skull interface (from 175% to 155%) and the skull-brain interface (from 142% to 118%).

Note that previous to this study the dose was prescribed to the 80% isodose contour for total scalp treatments at the M. D. Anderson Cancer Center, with no unusual complications observed. The modified technique showed suffi-

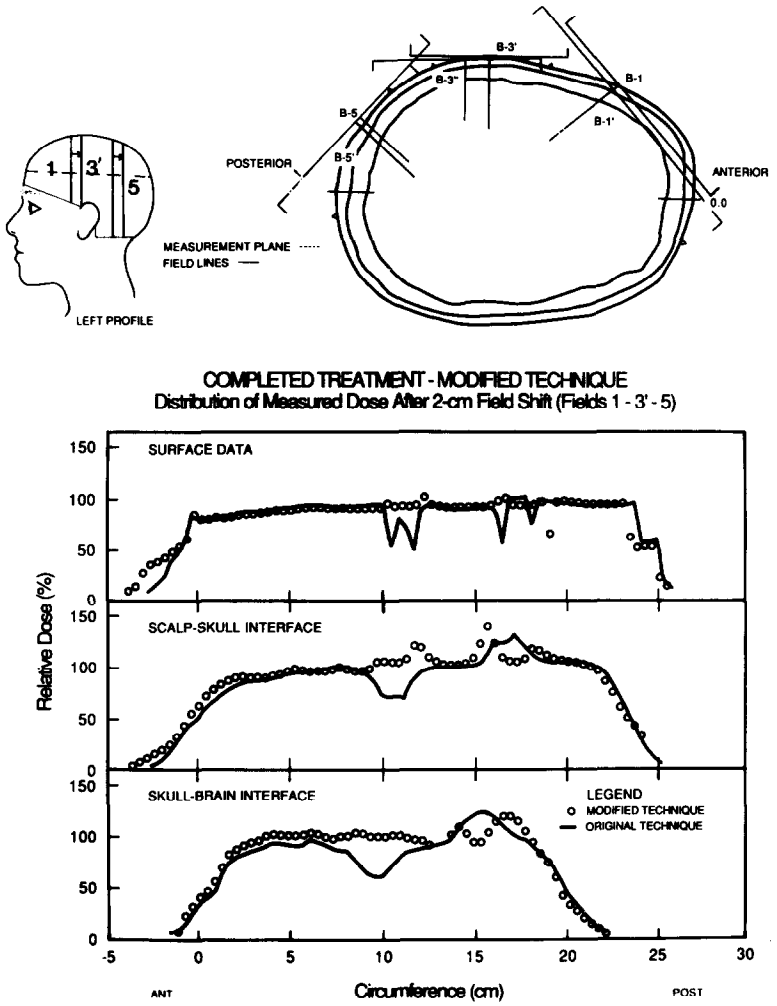

Fig. 6. Transverse plane dose distribution. Fields No. 1, 3′, and 5 were irradiated and then fields No. 1′, 3″, and 5′ after 2.0-cm field junction shift. Field lines are treated in fields No. 3′ and 3″. Film measurements made along circumference at surface, scalp-skull interface, and skull-brain interface. 7-MeV electrons; 6-mm acrylic at 98.9-cm source-to-acrylic distance; 100-cm SSD. Completed treatment — modified technique. The solid line shows the distribution resulting after the 1.0-cm field shift with the field lines not treated (original technique, Figure 3). The arrow indicates the field shift midway through the treatment.

cient dose at the surface and scalp-skull interface so that dose is now prescribed to the 95% isodose contour. This coupled with the moderate decrease in the maximum dose in the abuttment regions results in significantly less dose being delivered to the abuttment regions and to brain tissue, hence reducing the probability for complications. With treatment planning and calculated dose distributions, bolus thickness could be increased on an individual patient basis to further reduce the dose to the brain.

CONCLUSION

In summary, the modified total scalp electron irradiation technique includes the use of 6 fields with feathered edges, resulting in 12 unique electron fields, each requiring customized field shaping inserted in the standard applicator and a customized secondary skin shield conforming to the patient's head. A 7-MeV electron beam with 0.6 cm of acrylic bolus at 98.9 cm source-to-acrylic distance and a 100-cm SSD is used. The acrylic bolus decreases the dose gradient across the scalp by increasing the surface dose. Also, the practical range of the electrons is reduced to 2.7 cm, and the mean beam energy at the surface is 4.8 MeV. Initially, six fields encompassing the entire scalp are outlined on the patient. Each field is defined on the surface of the patient by customized secondary skin shielding. Field lines drawn in the sagittal plane are not included in any treatment field, whereas field lines drawn in the coronal plane are included in one of the treatment fields. In other words, a 3-mm gap is recommended along the sagittal border of abutted fields, and no gap is recommended along the coronal borders of abutted fields. All six fields

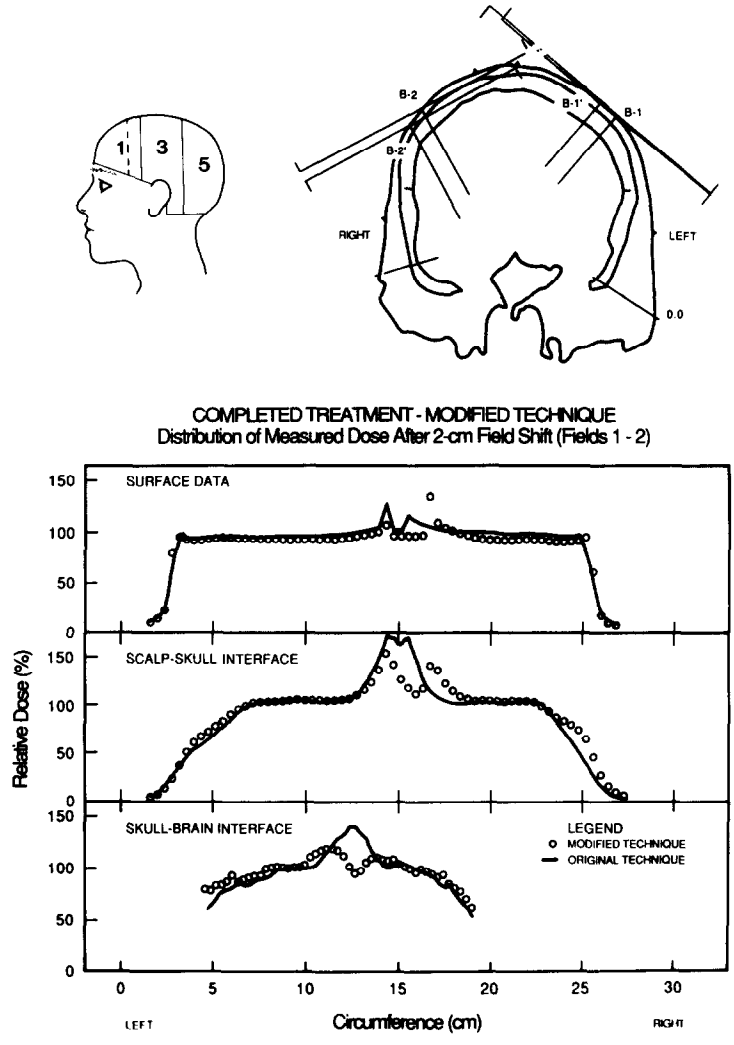

Fig. 7. Coronal plane dose distribution, fields No. 1 and 2 were irradiated and then fields No. 1′ and 2′ after 2.0-cm field junction shift. The field lines were not treated. Film measurements made along the circumference at the surface, scalp-skull interface, and skull-brain interface. 7-MeV electrons; 6-mm acrylic at 98.9-cm source-to-acrylic distance; 100-cm SSD. Completed treatment — modified technique. The solid line shows the distribution from the original technique, 1-cm shift, with neither field line treated (Figure 4).

are irradiated every treatment day. After 50% of the prescribed dose has been delivered the fields are shifted 2 cm. The prescribed dose is typically 50 Gy to 70 Gy over 5.5 to 6.5 weeks.

The original total scalp electron treatment protocol resulted in a nonuniform dose distribution to the scalp. Reasonably large variations, 50–170% of the prescribed dose delivered, occur in the field junction regions. The low doses were delivered because the field lines were not included in any treatment field, resulting in an approximately 3-mm gap between adjacent fields, while the angle of oblique incidence of each beam was not large enough to compensate for the lack of direct exposure. The 1-cm field junction shift did not adequately compensate for the dose heterogeneity, simply increasing the region of dose nonuniformity with little reduction in magnitude.

To ensure a minimum of 100% dose in the field junction regions, all field lines drawn in the coronal plane were included in a treatment field in our modified technique. However, all field lines drawn in the sagittal plane continued to be excluded from any treatment field since measurements indicated that the oblique beam incidence partially compensated for the approximately 3-mm gap between the fields. All field junction lines were shifted 2 cm after 50% of the prescribed dose had been delivered. This technique resulted in a significantly more uniform dose distribution, with the dose extremes being reduced to approximately 90% to 150%. The generally accepted threshold to brain dysfunction is 50 Gy to at least one-third of the brain (15, 18). In the modified technique the region receiving greater than 120% of the prescribed dose was slightly reduced, reducing the probability for clinical complications.

REFERENCES

1. AAPM Task Group 21. A protocol for the determination of absorbed dose from high energy photon and electron beams. Med. Phys. 10:741–771; 1983.
2. Able, C. M. Total scalp electron irradiation in the treatment of angiosarcoma (Thesis), University of Texas Health Science Center at Houston, 1987.
3. Almond, P. R. Radiation physics of electron beams. In: Tapley, N. D., ed. Clinical applications of the electron beam. New York: Wiley and Sons; 1976:10–22.
4. Antman, K. H.; Blum, R. H.; Wilson, R. E.; Corson, J. M.; Greenberger, J. S.; Amato, D. A.; Canellos, G. P.; Frei, E. Survival of patients with localized high-grade soft tissue sarcoma with multimodality therapy. Cancer 51:396; 1983.
5. Brooks, C. E. Management of soft tissue sarcomas. In: Uhthoff, H. K., Stahl, E., eds. Current concepts of diagnosis and treatment of bone and soft tissue tumors. Berlin: Springer; 1981:277–283.
6. Bruinvis, I. A. D.; Heukelom, S.; Mijnheer, B. J. Comparison of ionization measurements in water and polystyrene for electron beam dosimetry. Phys. Med. Biol. 30:1043–1053; 1985.
7. Constantinou, C. Tissue substitute for particulate radiation and their use in radiation dosimetry and radiotherapy (Dissertation), University of London, 1978.
8. Ekstrand, K. E.; Dixon, R. L. The problem of obliquely incident beams in electron-beam treatment planning. Med. Phys. 9:276–278; 1982.
9. Hodgkinson, D. J.; Soule, E. H.; Woods, J. E. Cutaneous angiosarcoma of the head and neck. Cancer 44:1106–1113; 1979.
10. Hogstrom, K. R.; Meyer, J. A. Electron beam characteristics of the Mevatron 77. Presented at the First International Users Conference, April 10–13, 1983, Pebble Beach, CA.
11. Hogstrom, K. R.; Mills, M. D.; Meyer, J. A.; Palta, J. R.; Mellenberg, D. E.; Meoz, R. T.; Fields, R. S. Dosimetric evaluation of a pencil-beam algorithm for electrons employing a 2-D heterogeneity correction. Int. J. Radiat. Oncol. Biol. Phys. 10:561–569; 1984.
12. International Commission on Radiation Units and Measurements. Radiation dosimetry: electron beams with initial energies between 1 and 50 MeV. Report No. 35. Washington, D. C.: ICRU Publications; 1984.
13. ICRP Task Group on Reference MAN. Report of the task group on reference man. ICRP Publication 23. New York: Pergamon Press; 1975.
14. Klevehagen, S. C. Physics of electron beam therapy. In: Lenihan, J. M. A., eds. Medical physics handbook, Vol. 13. Bristol: Adam Hilger Ltd. 1985:37–89.
15. Marks, J. E.; Baglan, R. J.; Prassad, S. C.; Blank, W. F. Cerebral radionecrosis: incidence and risk in relation to dose, time, fractionation and volume. Int. J. Radiat. Oncol. Biol. Phys. 7:243 252; 1981.
16. Matteson, L. O.; Nahum, A. E. L. Concerning comparisons of electron beam absorbed dose measurements in water and polystyrene. Med. Phys. 11:85–86; 1984.
17. Morales, P. H.; Lindberg, R. D.; Barkley, H. T. Soft tissue angiosarcomas. Int. J. Radiat. Oncol. Biol. Phys. 7:1655–1659; 1981.
18. Sheline, G. E.; Wara, W. M.; Smith, V. Therapeutic irradiation and brain injury. Int. J. Radiat. Oncol. Biol. Phys. 6:1215–1228; 1980.
19. Shiu, A. S.; Hogstrom, K. R. Dose in bone and tissue near bone-tissue interfaces for electron beams. Int. J. Radiat. Oncol. Biol. Phys. (In press) 1991.
20. Tapley, N. V. Skin and lips. In: Tapley, N. D., ed. Clinical applications of the electron beam. New York: Wiley and Sons, 1976, pp. 93–123.
21. White, D. R. Tissue substitute in experimental radiation physics. Med. Phys. 5:467–479; 1978.